High organic carbon burial but high potential for methane ebullition in the sediments of an Amazonian hydroelectric reservoir

Gabrielle R. Quadra[1]✉, Sebastian Sobek[2], José R. Paranaíba[1], Anastasija Isidorova[2], Fábio Roland[1], Roseilson do Vale[3], Raquel Mendonça[1]

[1] Laboratório de Ecologia Aquática, Programa de Pós-Graduação em Ecologia, Universidade Federal de Juiz de Fora, 36036 900, Brazil.

[2] Department of Ecology and Genetics, Limnology, Uppsala University, 752 36, Sweden.

[3] Universidade Federal do Oeste do Pará, Instituto de Engenharia e Geociências, 68040 255, Brazil.

✉gabrielle.quadra@ecologia.ufjf.br

Abstract

Reservoir sediments sequester significant amounts of organic carbon (OC), but at the same time, high amounts of methane (CH_4) can be produced and emitted during the degradation of sediment OC. While the greenhouse gases emission of reservoirs has received quite some attention, there is a lack of studies focusing on OC burial. In particular, there are no studies on reservoir OC burial in the Amazon, even though hydropower is expanding in the basin. Here we present results from the first investigation of OC burial and CH_4 concentrations in the sediments of an Amazonian hydroelectric reservoir. We performed sub-bottom profiling, sediment coring and sediment pore water analysis in the Curuá-Una reservoir (Amazon, Brazil) during rising and falling water periods. A spatially resolved mean sediment accumulation rate of 0.6 cm yr^{-1} and a mean OC burial rate of 91 g C m^{-2} yr^{-1} were found. This is the highest OC burial rate on record for low-latitude hydroelectric reservoirs, probably resulting from high OC deposition onto the sediment compensating for high OC mineralization at 28-30°C water temperature. Elevated OC burial was found near the dam, and close to major river inflow areas. C:N ratios between 10.3 and 17 (mean ± SD: 12.9 ± 2.1) suggest that both land-derived and aquatic OC accumulate in CUN sediments. About 23% of the sediment pore water samples had dissolved CH_4 above to saturation concentration, a higher share than in other hydroelectric reservoirs, indicating a high potential for CH_4 ebullition, particularly in river inflow areas.

Keywords: Amazon, carbon cycling, C:N ratio, dam, pore water, river inflow

Introduction

Although freshwater ecosystems represent a small fraction of the global area (~4% of terrestrial area) (Downing et al., 2012; Verpoorter et al., 2014), they play an important role in the global carbon cycle, emitting and burying carbon during transport from land to the oceans (Cole et al., 2007; Tranvik et al., 2009). Many studies have been conducted on inland water carbon emissions, while the organic carbon (OC) burial in inland water sediments is comparatively understudied (Raymond et al., 2013; Mendonça et al., 2017). Since a part of the buried OC may offset a share of greenhouse gas emission, it is essential to include OC burial in the carbon balance of inland water ecosystems (Kortelainen et al., 2013; Mendonça et al., 2017).

Freshwater OC burial rate varies both in space and time due to many factors, such as land cover, hydrological conditions, OC and nutrient input and climate change (Radbourne et al., 2017; Stratton et al., 2019). Several studies have shown that reservoirs bury more OC per unit area than lakes, rivers and oceans (Mulholland and Elwood, 1982; Mendonça et al., 2017), which may be attributed to the high sedimentation rate caused by the extensive sediment trapping when water flow is dammed (Vörösmarty et al., 2003). Considering the importance of reservoirs as a carbon sink (~40% of total inland water OC burial; Mendonça et al., 2017) and the increasing number of hydroelectric dams (Zarfl et al., 2015), the limited number of studies on OC burial in reservoirs severely hampers the understanding of this important component in the carbon balance of the continents (Mendonça et al., 2017). In particular, large regions of the Earth are at present completely unsampled concerning inland water carbon burial. Approximately 90% of the sites sampled for carbon burial are in North America and Europe, while there are only few measurements in South American, African and Asian countries (Mendonça et al., 2017).

To the best of our knowledge, OC burial has so far not been studied in an Amazonian reservoir. However, temperature and runoff were identified as important drivers of OC burial in lakes and reservoirs (Mendonça et al., 2017), and OC burial in Amazonian floodplain lakes was reported to be much higher than in other lakes (Sanders et al., 2017). These observations suggest that hydroelectric reservoirs in the Amazon area may bury OC at a comparatively high rate. Moreover, many new hydropower dams are planned in the Amazon due to the high potential of the area for hydroelectricity (da Silva Soito and Freitas, 2011; Winemiller et al., 2016). However, there is currently no data to gauge the potential effect of hydropower expansion in the Amazon on carbon burial.

On the other hand, it has been shown that reservoirs can be strong sources of methane (CH_4) to the atmosphere (Deemer et al., 2016). Several studies have shown a positive relationship between CH_4 production and temperature in freshwater ecosystems (Marotta et al., 2014; Wik et al., 2014; Yvon-Durocher et al., 2014; DelSontro et al., 2016; Aben et al., 2017), and also organic matter supply to sediment is an important regulator of CH_4 production and emission (Sobek et al., 2012; Grasset et al., 2018). Thus, tropical reservoirs, especially those situated in highly productive humid tropical biomes, such as the Amazon, may produce more CH_4 than temperate ones due to higher annual temperatures and availability of organic matter in their sediments (Barros et al., 2011; Mendonça et al., 2012; Fearnside and Pueyo, 2012; Almeida et al., 2013), even if highly-emitting reservoirs can also be situated in temperate regions (Deemer et al., 2016). Further, in many reservoirs, CH_4 ebullition (i.e., emission of gas bubbles) is an important or dominant emission pathway, but it is very difficult to measure due to its strong variability in space and time (McGinnis et al., 2006; Deemer et al., 2016). Measurements of dissolved CH_4 concentration in sediment pore water may, therefore,

help to identify if ebullition is likely to occur (CH_4 concentrations close to the sediment saturation), and thus to judge if the sediments act mainly as carbon sinks, or also as CH_4 sources.

Since both OC burial and CH_4 production take place in sediments and may potentially be high in reservoirs in the Amazon area, we conducted a study on the sediments of an Amazonian hydroelectric reservoir during hydrologically different seasons. Here we present the first spatially resolved OC burial estimate and mapping of CH_4 concentrations in sediment pore water in an Amazonian hydroelectric reservoir.

Material and methods

Study area

Curuá-Una is an Amazonian reservoir (CUN; 2°50′ S 54°18′ W) located in the Pará state (North of Brazil), created in 1977, and used mainly to produce energy. The mean water depth of CUN is 6 m (Fearnside, 2005; Paranaíba et al., 2018) and it has a maximum flooded area of 72 km^2 (Duchemin et al., 2000; Fearnside, 2005). The main tributary is the Curuá-Una River, contributing with most of the reservoir's water discharge (57.4%), but rivers Moju (11.7%), Mojuí (4.4%), Poraquê (3.2%) and other small ones (2.9%) are also important (Fearnside, 2005). The catchments of the largest tributaries, entering from the south, consist mainly of tropical rainforest, while the northwestern tributaries also contain a fraction (up to 41%) of managed land (Fig. 1).

The reservoir is characterized by a high amount of flooded dead trees (area with trees covers 90% of the total reservoir area), which may be expected to decrease water flow and promote sedimentation. According to a previous study (Paranaíba et al., 2018), CUN is oligotrophic (total nitrogen: 0.7 mg L^{-1}; total phosphorus: 0.02 mg L^{-1}), the

surface water is warm (30.1 ± 1.4 °C), slightly acidic (pH of 6.1 ± 0.7), with low conductivity (16 ± 11 μS cm^{-1}) and moderately oxygenated (6.7 ± 1.9 mg L^{-1}).

Sampling

We carried out two samplings in the CUN reservoir. In February 2016, during the rising water period (**Fig. S1**), we used an Innomar SES-2000 parametric sub-bottom profiler operating at 100 kHz (primary frequency) and 15 kHz (secondary frequency) to determine the bathymetry and sediment thickness (from which we planned to acquire spatially resolved sediment accumulation rates and OC burial rate, similar to Mendonça et al. 2014). Sediment thickness was difficult to observe with the sub-bottom profiler, though, presumably because of the widespread presence of gas bubbles in the sediment which reflect the sound waves very efficiently, preventing them from reaching the sub-bottom layer. Therefore, OC burial rates were determined from sediment cores only. In September 2017, during the falling water period (**Fig. S1**), additional sediment cores were then taken to cover the reservoir as much as possible.

We took a total of 114 sediment cores during the two sampling occasions, approximately evenly distributed along the reservoir, both longitudinally and laterally, to measure sediment thickness and, thus, estimate sediment accumulation and OC burial rates (**Fig. 1**, **Table S1**). Cores were retrieved using a gravity corer equipped with a hammer device (UWITEC, Mondsee, Austria) to sample the entire sediment layer, including the pre-flooding material. The layer of transition between post- and pre-flooding material was visually identified. Visual identification is possible because the moment when the reservoir was flooded is the onset of a lacustrine depositional regime, which is characterized by different sediment texture and composition in relation to the pre-flooding soil or fluvial sediment (**Fig. S2**). The thickness of the post-flooding

sediment was noted in all cores and used to calculate sediment accumulation rates (see 'data analysis'). Nineteen sediment cores, from sites spread out evenly over the reservoir, were sliced in 2 cm thick slices and dried at 40 ºC for further laboratory analysis. The samples were weighed before and after drying and the results are, then, expressed in dry weight.

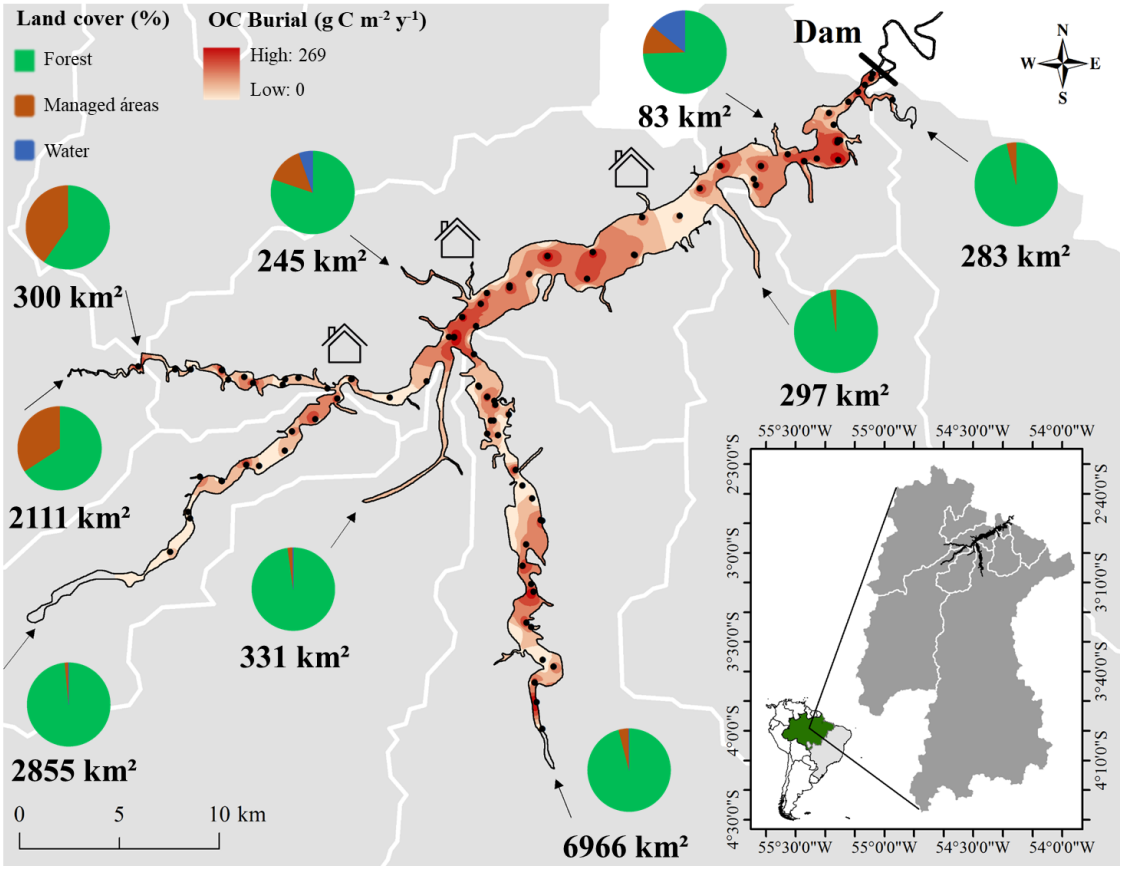

Figure 1. Organic carbon burial rate (OC burial; g C m^{-2} yr^{-1}) of the Curuá-Una reservoir. The circles show the land cover of each sub-catchment, delineated by white lines. The numbers near the circles show the area in km² for each sub-catchment. The black dots represent the sediment sampling sites to estimate OC burial rates. The arrows represent the main river inflows. The houses represent settlements at the reservoir. The bottom-right map shows the location of the reservoir in Brazil (the green area is the Brazilian Amazon region) and the total extension of each sub-catchment.

153 In both sampling campaigns, cores were taken for the analysis of pore water CH_4
154 concentration profiles (n = 16 in February 2016 and n = 9 in September 2017). Of the
155 nine cores taken in September 2017, eight were situated at sites previously sampled in
156 February 2016, to compare the CH_4 concentrations between sampling occasions. It is
157 difficult to sample the exact same location at different periods due to the water level
158 changes, GPS error and navigation. Thus, the repeated samplings at these eight sites
159 were within < 100 m distance.

160 Water temperature and dissolved oxygen profiles were measured with a
161 multiparameter sonde (YSI 6600 V2) in a total of 28 depth profiles, distributed across
162 the reservoir at both sampling occasions. Air pressure and temperature were measured
163 with a portable anemometer (Skymaster SpeedTech SM-28, accuracy: 3%), water depth
164 was measured with a depth gauge (Hondex PS-7), and sediment temperature with a
165 thermometer (Incoterm), which was inserted into the sediment right after core retrieval.

166 *Carbon and nitrogen analysis*

167 OC and total nitrogen (TN) concentrations were determined in a sub-set of 19
168 cores, distributed evenly across the reservoir area. In each of these cores, the first and
169 second layers (0 to 4 cm deep, containing the fresher OC), the last sediment layer above
170 the pre-flooding soil surface (containing the older OC) and one sample every ~8 cm in
171 between (OC of intermediate age) were analyzed. This selection of layers for C and N
172 analyses was motivated by the exponential decrease of OC mass loss rates during
173 sediment degradation (Middelburg et al., 1993; Gälman et al., 2008). Linear
174 interpolation was used to derive OC and TN concentrations of layers that were not
175 measured.

Dried sediment samples were ground in a Planetary Ball Mill (Retsch PM 100) equipped with stainless steel cup and balls. Sediment was packed in pressed tin capsules and analyzed for TC and TN with a Costech 4010 elemental analyzer. The molar C:N ratio in the surface layers was then calculated. The presence of carbonates was checked in the samples qualitatively by adding drops of acid and checking visually for reaction. No evidence of solid carbonates was found, thus measurements of TC correspond to OC.

CH_4 concentration in pore water

The CH_4 concentration in pore water was measured (according to Sobek et al., 2012 and Mendonça et al., 2016) to determine if CH_4 is close to saturation concentration and, thus, prone to form gas bubbles. The presence of gas bubbles is indicative for an elevated probability of CH_4 ebullition, but not necessarily relates quantitatively to ebullition flux, since ebullition flux to the atmosphere is also dependent on water depth, sediment grain size, and pressure fluctuations (McGinnis et al., 2006; Maeck et al., 2014; Liu et al., 2016). The top 20 cm (February 2016) or 40 cm (September 2017) of the sediment cores were sampled every 2 cm. Deeper sediment was sampled every 4 cm until the bottom or pre-flooding material. Using a core liner with side ports, 2 ml of sediment were collected using a syringe with a cut-off tip, added to a 25 mL glass vial with 10 ml of distilled water, and closed with a 10 mm thick butyl rubber stopper. The slurry (2 mL sediment + 10 mL distilled water) was equilibrated with 13 mL headspace of ambient air (void volume of the glass vial) immediately after sampling by vigorously shaking the glass vial, and then the headspace was transferred to another syringe. The headspace was stored in the syringe, closed with a gas-tight valve, and then injected into the analyzer within the same day. The headspace CH_4 concentration was measured by an Ultraportable Greenhouse Gas Analyzer (UGGA,

Los Gatos Research) with a custom-made sample injection port, and the peaks were integrated using R software (RStudio Version 1.1.383). The CH_4 concentration in the pore water was calculated from the headspace CH_4 concentration, based on the Henry's law constants. The saturation concentration of CH_4 in each sediment layer was calculated based on air pressure, water depth, sediment temperature, and sample depth within the sediment core. The sediment layers with CH_4 concentrations above 100% saturation were considered as prone to ebullition. This is a conservative assumption because it is likely that a part of the CH_4 in the sediment is lost to the atmosphere due to pressure drop during core retrieval, as well as during sample processing.

Data analysis

The average sediment accumulation rate (SAR; cm yr^{-1}) was calculated for each of the 114 cores by dividing the thickness of the post-flooding sediment by the years since the reservoir construction (39 years in 2016 or 40 years in 2017), according to the equation:

$$Sediment\ accumulation\ rate = \frac{\text{sediment thickness}}{\text{reservoir age}}$$

This approach returns the average sediment accumulation rate over the lifetime of the reservoir (Renwick et al., 2005; Kunz et al., 2011; Mendonça et al., 2014; Quadra et al., 2019), and therefore includes short-term variability in sediment deposition, for example, caused by an episodic change in sediment load or internal sediment movement. The large amount of core samples distributed evenly across the reservoir body also covers the spatial variability in sediment deposition, for example due to sediment focusing (sediment movement with preferential deposition in deeper areas).

OC burial rates (g C m^{-2} yr^{-1}) were calculated for the sub-set of 19 sites where OC content was analyzed. OC mass (g C) in each sediment slice was calculated as OC content (g C g^{-1}) multiplied by dry sediment mass (g). Total OC mass (g C) in the cores was the sum of OC mass in all post-flooding sediment layers. Then, the OC burial rate (g C m^{-2} yr^{-1}) for each of these 19 sites was calculated using the total OC mass (g C), core surface area (2.8 x 10^{-3} m^2) and the reservoir age at the sampling dates, according to the equation:

$$Organic\ carbon\ burial\ rate = \frac{\text{Organic carbon mass in the post} - \text{flooding sediment}}{\text{core area} * \text{reservoir age}}$$

SAR was positively correlated to OC burial rate in the sites (see Results; y = 159.03x - 4.4212; R^2 = 0.87; **Fig. S3**), and we used this regression equation to estimate the OC burial rate (g C m^{-2} yr^{-1}) for the remaining 95 coring sites where OC content was not analyzed.

The SAR and OC burial rates from the 114 cores were then interpolated to the reservoir area using the Inverse Distance Weighted algorithm (IDW, cell size of approximately 22 m x 22 m), producing spatially resolved maps of SAR, OC burial rate. From the spatially-resolved average OC burial rate, the reservoir age (40 years) and total flooded area (72 km^2), we calculated the total OC stock in the reservoir sediment. Using the same approach, we interpolated the pore water CH_4 concentration, and C:N ratio for the whole reservoir area. Spatial analyses were performed in ArcGIS 10.3.1 (ESRI).

In order to investigate any potential relationships between the land cover of sub-catchments and the spatial distribution of sediment characteristics and rates, land cover data was derived from maps of 1 km resolution (Global Land Cover Project, GLC2000),

made available by the European Commission's science and knowledge service, including 23 land cover classes. The classes found in the CUN watershed were then grouped in three main classes: (1) forest (tree cover, natural vegetation, shrub, and herbaceous cover); (2) managed areas (cultivated and managed areas, cropland and bare areas); (3) and water bodies. The extent of the CUN watershed and sub-catchments were identified using the WWF HydroBASINS tool (HydroSHEDS, 2019).

Results

Water column profiles

The water column temperature profiles showed a mean of 30 ± 1 ºC, 29 ± 1 ºC and 29 ± 2 ºC in the surface, the middle and bottom layer, respectively. The dissolved oxygen average was 7 ± 1 mg L^{-1}, 6 ± 1 mg L^{-1} and 5 ± 1 mg L^{-1} in the surface, the middle and bottom layer, respectively. These water profiles suggest that the relatively shallow water column does not develop stable stratification over any extended periods of time, even if short-lived stratification events can occur (**Table S2**).

Sediment accumulation and organic carbon burial rates

SAR in the coring sites (n = 114) varied from 0 to 1.7 cm yr^{-1} (mean ± SD of 0.6 ± 0.4 cm yr^{-1}, **Table S1**). In some areas of rocky or sandy bottom, especially near river inflows and along the main river bed, sediment could not be retrieved with our corer and SAR was considered as zero (total of 10 sites). OC burial rate in the coring sites (n = 114) varied from 0 to 269 g C m^{-2} yr^{-1} (mean ± SD of 91 ± 61 g C m^{-1} yr^{-1}, **Table S1**). The highest values of OC burial were observed near the dam, at the confluence of the major inflowing rivers, and in the inflow area of the main tributary, Curuá-Una River (**Fig. 1**). Our sampling was representative of the whole system, from the margins, where

there is a greater presence of dead tree trunks, to the river bed, where the sedimentation was lower (**Fig. 1**). Therefore, the simple mean OC burial from the cores resulted in the same mean OC burial rate derived from the spatial interpolation (91 g C m^{-1} yr^{-1}). The total burial rate for the CUN reservoir area was 6.5 x 10^{10} g C yr^{-1}, corresponding to an accumulation of 0.3 Tg C in CUN sediments since its construction.

C:N ratio and land cover

The C: N ratio of the surface layers of sediment (n = 19), used as an indicator of organic matter source, varied from 10.3 to 17 (average ± SD of 12.9 ± 2.1, **Table S3**). Higher C:N ratios were observed in the dam area and at the river inflows (**Fig. 2**). Tropical rain forest is the dominant land cover in CUN, covering 90.8% of the watershed, followed by managed areas (8.9%) and water (0.3%) (**Table S4**).

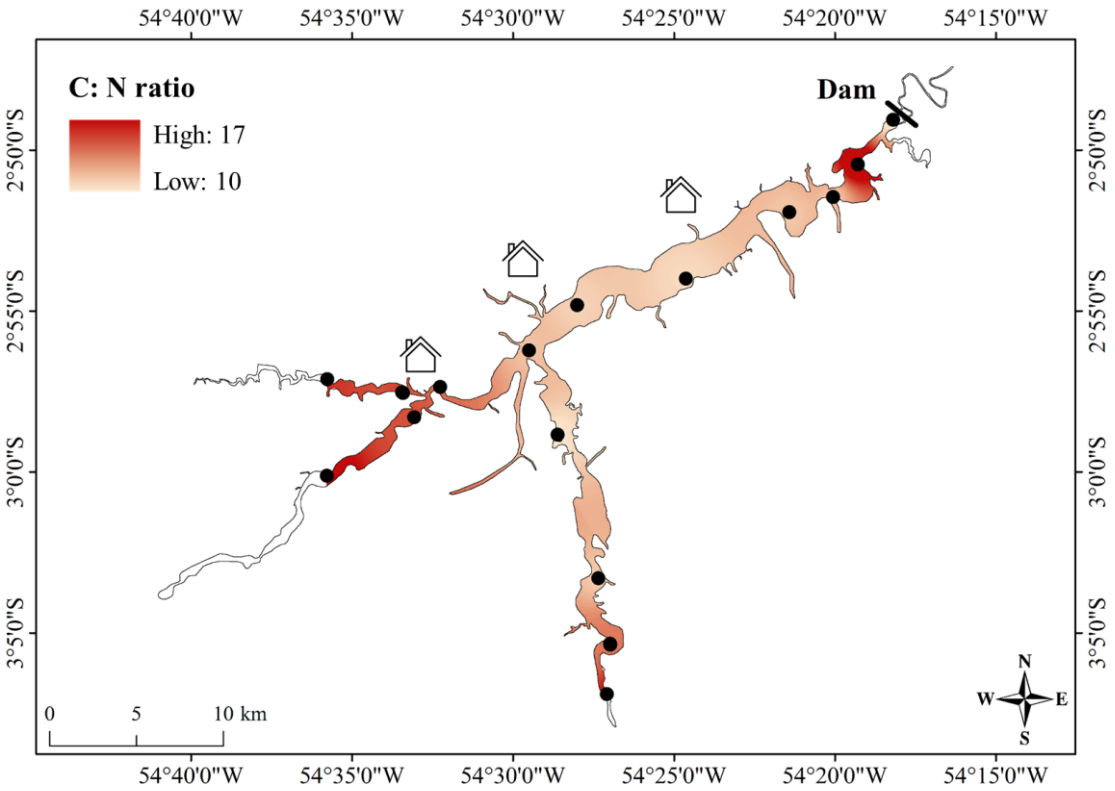

Figure 2. C:N ratio of surface sediment in Curuá-Una reservoir. The black dots represent the sampling sites. The houses represent the settlements at the reservoir.

Pore water CH_4 profiles and saturation

The overall mean CH_4 concentration in pore water from CUN was 1,729 ± 1,939 µM of CH_4 (mean ± SD) with similar averages during rising (1,700 ± 1,637 µM of CH_4, **Fig. S4**) and falling water (1,764 ± 2,243 µM of CH_4, **Fig. S4**) periods. At eight sites, we could make paired observations of CH_4 concentration in sediment pore water at both rising and falling periods (**Fig. 3**). These data show that the seasonal difference of CH_4 concentration in pore water was low and not significant (t-test, $t(14) = -0.08$, $p = 0.94$). Of the 25 pore water CH_4 profiles, 20 contained at least one sample with pore water CH_4 above the 100% saturation concentration; of the total of 386 pore water samples, 90 samples (23%) were above the CH_4 saturation concentration. This indicates a high likelihood of gas bubble formation in the majority of the sampled sites, and thus the possibility of CH_4 ebullition (**Table S5**). Pore water CH_4 saturation was higher in river inflow areas, especially in sampling sites in the Curuá-Una main river. The confluence of the rivers and the dam area were also characterized by high pore water CH_4 (**Fig. 4**). The widespread appearance of gas bubbles in the sediment is in accordance with the sub-bottom profiler data, which for a large part of the reservoir could not be used to identify sub-bottom structures, because of a very strong acoustic reflector in surficial sediment, presumably gas bubbles.

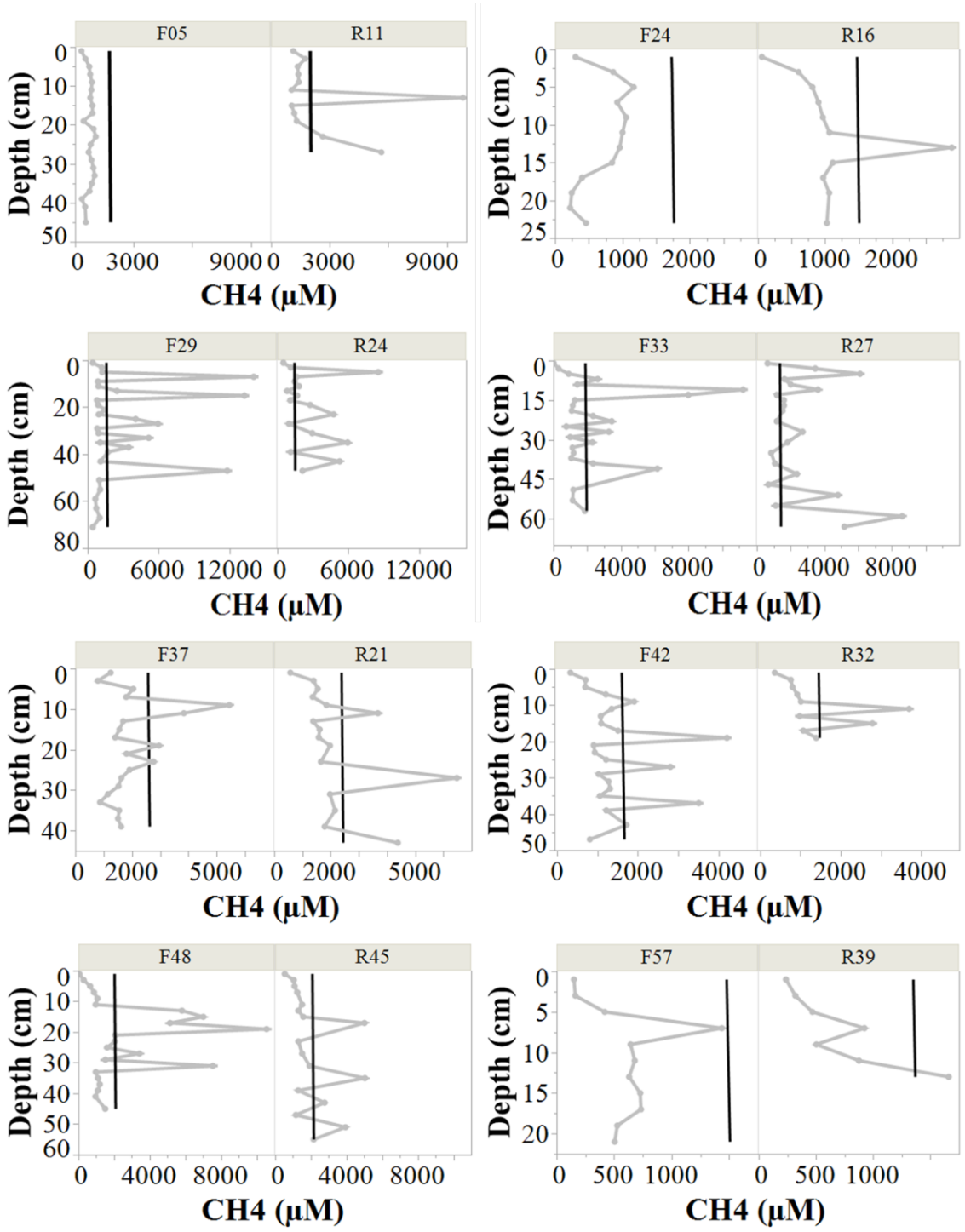

301

302 **Figure 3.** Paired observations of pore water CH_4 profiles during rising (R) and falling

303 (F) water periods at eight different sampling sites across the reservoir. Black lines

304 represent the CH_4 saturation line (µM) and grey lines represent the measured CH_4

305 concentration (µM) over sediment depth.

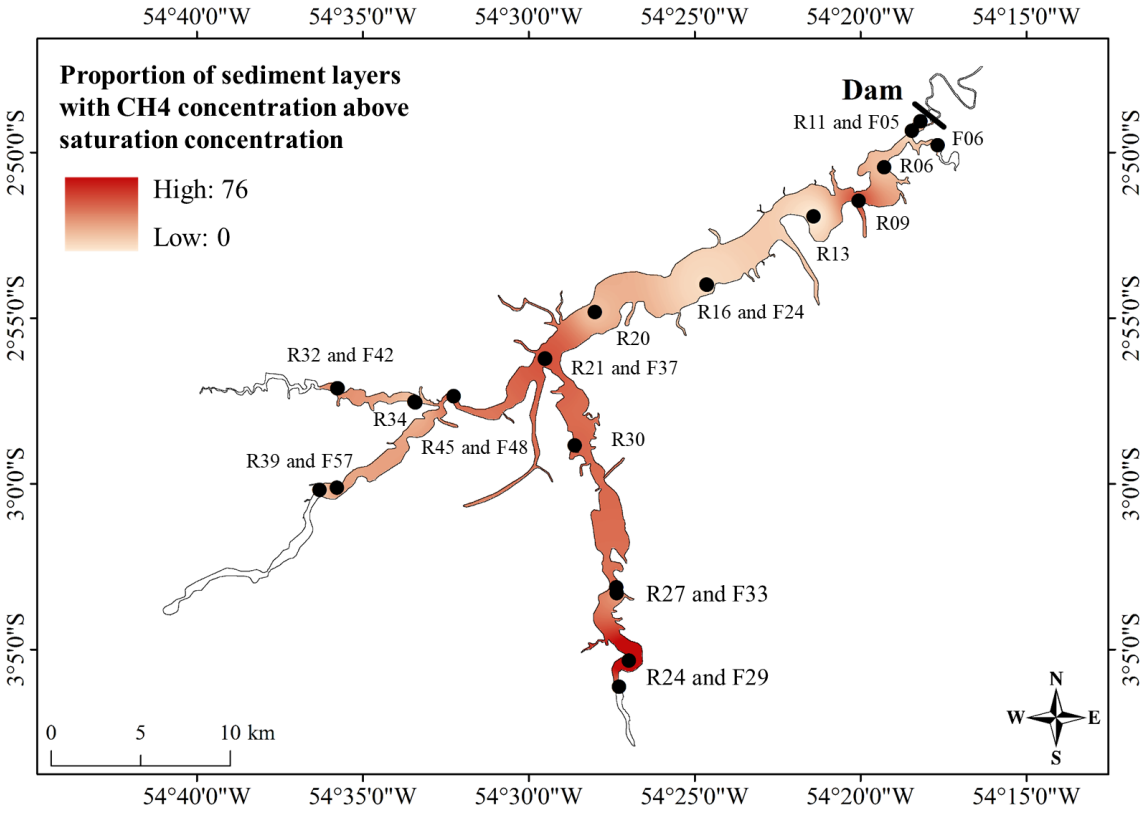

Figure 4. Percentage of sediment layers with CH_4 concentration above saturation. The black dots represent the sampling sites to produce the interpolation. The houses represent the settlements at the reservoir.

Discussion

SAR and OC burial in an Amazonian reservoir

When a river enters a reservoir, the water flow tends to decrease, favoring the deposition of suspended particles (Fisher, 1983; Scully et al., 2003). Typically, reservoir sedimentation rates are higher in the inflow areas and lower near the shores (Morris and Fan, 1998; Sedláček et al., 2016). CUN showed high SAR near the inflow areas, especially in the main tributary, but in contrast to other reservoirs (e.g. Mendonça et al., 2014), we did not observe any decrease in SAR towards the margins. In CUN, sediment accumulation across the entire reservoir area is favored by the shallow topography of

319 the area, and by the presence of dead tree trunks along the reservoir including the
320 margins, which reduce water flow and wave-driven resuspension. Accordingly, our data
321 show that SAR was randomly distributed in relation to the water column depth (**Fig.**
322 **S5**). Some reservoirs show higher sedimentation rates near the dam, which can be called
323 'muddy lake area' (Morris and Fan, 1998; Sedláček et al., 2016), and occurs in
324 reservoirs where the fine sediment is transported all the way to the dam (Morris and
325 Fan, 1998; Jenzer Althaus et al., 2009; Sedláček et al., 2016; Schleiss et al., 2016). CUN
326 may be one of those cases (**Fig. 1**), possibly because water retention time is low in the
327 main river channel which is narrow and well separated from the dead tree area,
328 permitting transport of fine-grained sediment until the deeper dam area (**Fig. S6**), where
329 sediments tend to accumulate (Lehman, 1975; Blais and Kalff, 1995). Sediment
330 accumulation was also high at the confluence of the three main tributaries (**Fig. 1**),
331 probably due to sediment deposition as water flow slows down when the rivers enter the
332 main body of the reservoir.

333 Although average SAR in CUN (0.6 cm yr^{-1}) was only slightly higher than that
334 of non-Amazonian reservoirs in Brazil (e.g. Mendonça et al., 2014: 0.5 cm yr^{-1};
335 Franklin et al., 2016: 0.4 cm yr^{-1}), OC burial rates were much higher in CUN than in
336 other hydroelectric reservoirs in the tropics and sub-tropics . For example, OC burial
337 was four times lower in Lake Kariba (23 g C m^{-2} yr^{-1}, Zimbabwe, Kunz et al., 2011) and
338 about two times lower in Mascarenhas de Moraes (42 g C m^{-2} yr^{-1}, Brazil, Mendonça et
339 al., 2014) and other Brazilian reservoirs (40 ± 28 g C m^{-2} yr^{-1}, Brazil, Sikar et al., 2009)
340 when compared to CUN. Even though natural lakes tend to bury OC at lower rates than
341 artificial reservoirs (Mendonça et al., 2017), some Amazonian floodplain lakes showed
342 higher OC burial rates than the CUN reservoir (266 ± 57 g C m^{-2} yr^{-1}; Sanders et al.,
343 2017). This is probably due to their smaller sizes which may result in a higher SAR

since there is little area for sediment deposition, but high sediment load from the river during periods of high discharge. While a comparison with the latest global estimate of OC burial in reservoirs – median of 291 g C m^{-2} yr^{-1} (Mendonça et al., 2017) may lead to the conclusion that OC burial in CUN is low, it must be accounted that this global estimate (Mendonça et al., 2017) includes many small agricultural reservoirs (farm ponds), which are generally highly eutrophic systems that receive high sediment inputs from agriculture, resulting in extremely high OC burial rates (Downing et al., 2008). Hence, if compared to other hydroelectric reservoirs at low latitudes, our conclusion remains that OC burial in CUN is high. Importantly, comparisons of mean SAR and OC burial rate between studies may be complicated by different sampling schemes, as sedimentation can vary in space and time (Radbourne et al., 2017; Stratton et al., 2019); for example, while in some studies, sites along the margins with zero sedimentation were sampled (e.g. Mendonça et al., 2014; our study), in other studies it was not (Moreira-Turcq et al., 2004; Knoll et al., 2014).

The high OC burial in CUN when compared to other low-latitude hydroelectric reservoirs is probably due to the high OC inputs from the productive Amazonian rain forest (Zhang et al., 2017), which compensates the intense sediment mineralization rates caused by high temperature. Using the linear regression model from a compilation of mineralization in freshwater sediments from the literature (OC mineralization = 1.52 + 0.05 x temperature; Cardoso et al., 2014) and the mean temperature of the bottom water in CUN (29°C), sediment OC mineralization is estimated at 325 g C m^{-2} yr^{-1}. This estimate of the sediment mineralization rate is in the upper end of the range of values found for Brazilian reservoirs (Cardoso et al., 2014), but may even be conservative given that the CUN reservoir is located in a highly productive biome with high organic matter supply. The total OC deposition rate onto the sediment (OC mineralization + OC

burial) of CUN is thus 418 g C m^{-2} yr^{-1}, returning a OC burial efficiency of 22 % (OC burial efficiency = OC burial / OC deposition rate; Sobek et al., 2009). As expected, due to the positive effect of temperature on mineralization, the estimated OC burial efficiency in the CUN reservoir is low in comparison to other reservoirs (at least 41% in the tropical lake Kariba (Kunz et al., 2011); mean of 67% in the sub-tropical Mascarenhas de Moraes reservoir (Mendonça et al., 2016); mean of 87% in the temperate lake Wohlen reservoir (Sobek et al., 2012)). A low OC burial efficiency allows high OC burial only if OC deposition onto the sediment is high enough, and we suggest that the high productivity of the surrounding Amazonian rainforest constitutes a strong OC supply to CUN sediments.

The C:N ratio indicates that the sediment OC in CUN consists of a mixture of land-derived and internally-produced OC. The surface sediment C:N ratio varied from 10.3 to 17.0 (**Table S3**), and the C:N ratios of phytoplankton are typically 6-9, of aquatic macrophytes >10, of land plants >40 (Meyers and Ishiwatari, 1993; Grasset et al., 2019) and of Amazonian topsoils 10 to 14 (Batjes and Dijkshoorn, 1999). Higher C:N values at the river inflow areas (**Fig. 2**) may indicate input from the highly productive watershed and thus the high load of land-derived OC to the sediment. Tropical rain forest is the dominant land cover in the CUN catchment (91%, **Table S4**), which may suggest that that the high OC burial rates in CUN are related to a high OC input from the watershed. However, probably due to the strong effect of SAR on OC burial, there was no strong relation between OC burial rate and C:N ratio (**Fig. S7A**), even though the C:N ratio has been shown to affect the OC burial efficiency (Sobek et al., 2009). In addition, the middle section of the reservoir was characterized by relatively low C:N ratio, indicating a significant share of aquatic OC in the sediment (**Fig. 2**). Likely, the higher water transparency downstream from the river inflow areas

394 due to particle settling stimulate aquatic primary production. Possibly, also sewage
395 input from riverside communities (represented as houses in **Fig. 2**) contributes with N to
396 the reservoir and thus further stimulates aquatic production, since a comparatively low
397 C:N ratio was found near these settlements. Also, even at low C:N ratios, OC burial
398 rates were high (**Fig. S6A**). Hence, it is evident that internally-produced OC makes up
399 an important contribution to the OC buried in the sediments of CUN. The source of
400 buried OC has an important implication in terms of accounting for the sediment carbon
401 as a new sink or not (Prairie et al., 2017); however, our data do not allow us to make a
402 quantitative estimate of the share of the CUN sediment carbon stock that is of aquatic
403 origin, and thus may be accountable as a new carbon sink resulting from river damming
404 (Prairie et al., 2017).

405 The spatial pattern of OC burial suggests that the catchment size affects
406 sediment load and sedimentation, since the largest sub- catchment n (6966 km^2),
407 entering CUN from the south, corresponds with high OC burial rates in the southern
408 river inflow area (**Fig. 1**). The northwestern tributaries, which drain only 2111 and 300
409 km^2, are not associated with high OC burial in the northeastern tributary (**Fig. 1**),
410 possibly because they are smaller, even though they have a higher share of managed
411 land (34 and 41%, respectively) than the southern sub-catchment (4%). Apparently,
412 even though land management is known to increase erosion (Syvitski and Kettner,
413 2011), we cannot detect any such effect on sediment OC burial. Also concerning the
414 C:N ratio, an effect of land cover is not evident, since the inflow area of the forest-
415 dominated sub-catchment in the southwest (2855 km^2; 99% forest) had a similar C:N
416 ratio as the tributary of the northwestern sub-catchments, with their higher share of
417 managed land. Possibly, the effect of land cover is masked by other factors affecting
418 sediment OC and C:N, such as internal productivity and local particle settling patterns.

Despite being high compared to other hydroelectric reservoirs, OC burial in CUN represents only 15% of the total carbon emission to the atmosphere reported for the CUN reservoir (509 g C m^{-2} yr^{-1}, Duchemin et al., 2000). Similarly, a study conducted in a boreal Canadian reservoir found that OC burial corresponded to 10% of reservoir C emission (Teodoru et al., 2012), although burial in other reservoirs can be close to (70%, Mendonça et al., 2014) or even much higher than the total carbon emission to the atmosphere (1600%, Sobek et al., 2012). The magnitudes of carbon burial in relation to the emission in reservoirs depends on many factors (Mendonça et al., 2012). Therefore, although freshwater carbon emission tends to be consistently higher than OC burial in Amazonian freshwater systems (Mendonça et al., 2012), we cannot speculate in how far the results of this study applies to other reservoirs in the Amazon region since many factors affect the carbon processing in inland waters.

High potential for CH_4 ebullition

Sites with higher OC burial rate, i.e. river inflow areas, especially the Curuá-Una river, the confluence of the three main rivers and the dam area, also showed a tendency towards higher extent of CH_4 saturation (**Fig. 5**). Hence, the CH_4 production in CUN sediments may rather be driven by the OC supply rate to anaerobic sediment layers than by the reactivity of the sediment OC, since there was no association between the C:N ratio and the extent of CH_4 saturation (**Fig. S7B**). Links between high sedimentation rate and sediment CH_4 pore water concentration as well as CH_4 ebullition have been reported previously (Sobek et al., 2012; Maeck et al., 2013), and in addition, fresh land plant-derived organic matter such as leaves transported by the rivers may fuel substantial CH_4 production at anoxic conditions (Grasset et al., 2018). This highlights that sediment accumulation bottoms close to river inflow areas can be prone to exhibit

high CH_4 ebullition (DelSontro et al., 2011), not least because the shallow water column in inflow areas (**Fig. S6**) facilitates CH_4 bubble transport to the atmosphere.

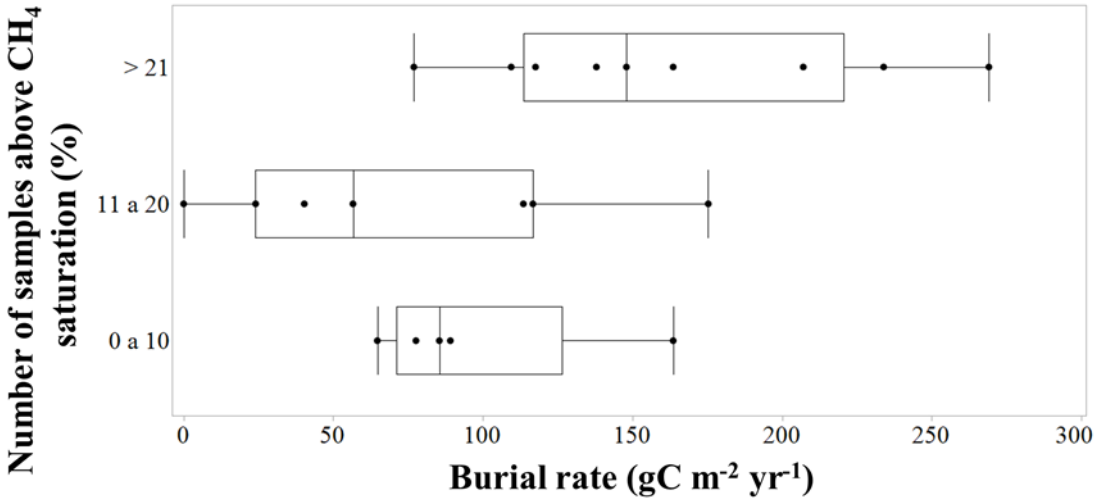

Figure 5. Boxplot of percentage of sediment layers with CH4 concentration above saturation and OC burial rate.

Compared to other reservoirs, CUN had a higher share of sites (20 of 25) with pore water CH_4 concentration over the saturation threshold. In the Mascarenhas de Morais reservoir (Brazil), 6 of 16 sites with pore water CH_4 concentration over the saturation threshold were found (Mendonça et al., 2016). In Lake Wohlen (Switzerland), 4 of 8 sites with pore water CH_4 concentration over the threshold were found (Sobek et al., 2012). Using the 100% saturation concentration as a threshold may underestimate the potential for ebullition, since changes in the pressure may result in bubbles release during sediment sampling, especially in layers above 100% saturation. Therefore, our results of the degree of pore water CH_4 saturation, as well as the results from the literature cited above, are conservative.

We did not find statistical difference between CH_4 pore water concentration during rising and falling periods (**Fig. 3**), although other studies suggest a strong

influence of water level or pressure changes on CH_4 ebullition (Mattson and Likens, 1990; Eugster et al., 2011; Maeck et al., 2014). Interestingly, 2 of the 8 sites with generally low CH_4 pore water concentration were low at both sampling occasions, indicating that there may be an important spatial component in sediment CH_4 production and saturation (**Fig. 3**, sites F24 x R16 and F57 x R39), which however was not related to the C:N ratio or OC burial rate at these sites.

Conclusions

The comparatively high OC burial rate of the Amazonian CUN reservoir probably results from high OC deposition onto the sediment, since the warm water (28-30°C) implies a high sediment OC mineralization rate. The forest seems to be a major OC source to the reservoir although the relatively low C:N ratio in large parts of the reservoir indicates a significant aquatic contribution to sediment OC burial. In some parts of the reservoir, particularly in the river inflow areas, sediments are probably a CH_4 source by ebullition. Therefore, large inputs from a highly productive forest probably boost the OC burial rate, as well as CH_4 production, with a still unknown net effect. Given the planned expansion of hydropower dams in the Amazon region, future studies should quantify how OC burial and CH_4 emission may be affected by new Amazonian hydroelectric reservoirs.

Data availability. All the data used in this study can be found in the manuscript and in the Supplement.

Author contributions. GRQ, JRP, AI, RM, RV carried out the sampling campaings. GRQ processed the data. AI analyzed the samples. GRQ and JRP prepared the figures. RM, SS, FR designed the study. All authors contributed to interpreting data and writing the manuscript.

Competing interests. The authors declare that they have no conflict of interest.

Acknowledgments. The research leading to these results has received funding from the European Research Council under the European Union's Seventh Framework Programme (FP7/2007–2013)/ERC grant agreement n° 336642. S.S. received additional support by the program *Pesquisador Visitante Especial*, *Ciência sem Fronteiras*, n° 401384/2014-4. This study was also financed in part by the *Coordenação de Aperfeiçoamento de Pessoal de Nível Superior* (CAPES) - Finance Code 001. F.R. has been supported by the *Conselho Nacional de Desenvolvimento Científico e Tecnológico* (CNPq; grant no. 401384/2014-4). We are thankful for the support from ELETRONORTE during the field campaigns.

References

Aben, R. C., Barros, N., Van Donk, E., Frenken, T., Hilt, S., Kazanjian, G., Lamers, L. P., Peeters, E. T., Roelofs, J. G., and de Senerpont Domis, L. N.: Cross continental increase in methane ebullition under climate change, Nature communications, 8, 1682, 2017.

Almeida, R. M., Barros, N., Cole, J. J., Tranvik, L., and Roland, F.: Emissions from Amazonian dams, Nature Climate Change, 3, 1005, 2013.

Barros, N., Cole, J. J., Tranvik, L. J., Prairie, Y. T., Bastviken, D., Huszar, V. L., Del Giorgio, P., and Roland, F.: Carbon emission from hydroelectric reservoirs linked to reservoir age and latitude, Nature Geoscience, 4, 593, 2011.

Batjes, N. H., and Dijkshoorn, J. A.: Carbon and nitrogen stocks in the soils of the Amazon Region, Geoderma, 89, 273-286, 1999.

Blais, J. M., and Kalff, J.: The influence of lake morphometry on sediment focusing, Limnology and Oceanography, 40, 582-588, 1995.

Cardoso, S. J., Enrich-Prast, A., Pace, M. L., and Roland, F.: Do models of organic carbon mineralization extrapolate to warmer tropical sediments?, Limnology and Oceanography, 59, 48-54, 2014.

Cole, J. J., Prairie, Y. T., Caraco, N. F., McDowell, W. H., Tranvik, L. J., Striegl, R. G., Duarte, C. M., Kortelainen, P., Downing, J. A., and Middelburg, J. J.: Plumbing the global carbon cycle: integrating inland waters into the terrestrial carbon budget, Ecosystems, 10, 172-185, 2007.

da Silva Soito, J. L., and Freitas, M. A. V.: Amazon and the expansion of hydropower in Brazil: Vulnerability, impacts and possibilities for adaptation to global climate change, Renewable and Sustainable Energy Reviews, 15, 3165-3177, 2011.

Deemer, B. R., Harrison, J. A., Li, S., Beaulieu, J. J., DelSontro, T., Barros, N., Bezerra-Neto, J. F., Powers, S. M., Dos Santos, M. A., and Vonk, J. A.: Greenhouse gas emissions from reservoir water surfaces: a new global synthesis, BioScience, 66, 949-964, 2016.

DelSontro, T., Boutet, L., St-Pierre, A., del Giorgio, P. A., and Prairie, Y. T.: Methane ebullition and diffusion from northern ponds and lakes regulated by the interaction between temperature and system productivity, Limnology and Oceanography, 61, S62-S77, 2016.

DelSontro, T., Kunz, M. J., Kempter, T., Wüest, A., Wehrli, B., and Senn, D. B.: Spatial heterogeneity of methane ebullition in a large tropical reservoir, Environmental science & technology, 45, 9866-9873, 2011.

Downing, J. A., Cole, J. J., Duarte, C., Middelburg, J. J., Melack, J. M., Prairie, Y. T., Kortelainen, P., Striegl, R. G., McDowell, W. H., and Tranvik, L. J.: Global abundance and size distribution of streams and rivers, Inland waters, 2, 229-236, 2012.

Downing, J. A., Cole, J. J., Middelburg, J. J., Striegl, R. G., Duarte, C. M., Kortelainen, P., Prairie, Y. T., and Laube, K. A.: Sediment organic carbon burial in agriculturally eutrophic impoundments over the last century, Global Biogeochemical Cycles, 22, 2008.

Duchemin, É., Lucotte, M., Canuel, R., Queiroz, A. G., Almeida, D. C., Pereira, H. C., and Dezincourt, J.: Comparison of greenhouse gas emissions from an old tropical reservoir with those from other reservoirs worldwide. Internationale Vereinigung für theoretische und angewandte Limnologie: Verhandlungen, 27, 1391-1395, 2000.

Eugster, W., DelSontro, T., and Sobek, S.: Eddy covariance flux measurements confirm extreme CH_4 emissions from a Swiss hydropower reservoir and resolve their short-term variability. Biogeosciences, 8, 2815-2831, 2011.

Fearnside, P. M., and Pueyo, S.: Greenhouse-gas emissions from tropical dams, Nature Climate Change, 2, 382, 2012.

Fearnside, P. M.: Do hydroelectric dams mitigate global warming? The case of Brazil's Curuá-Una Dam, Mitigation and Adaptation Strategies for Global Change, 10, 675-691, 2005.

Fisher, R. V.: Flow transformations in sediment gravity flows, Geology, 11, 273-274, 1983.

Franklin, R. L., Fávaro, D. I. T., and Damatto, S. R.: Trace metal and rare earth elements in a sediment profile from the Rio Grande Reservoir, Sao Paulo, Brazil: determination of anthropogenic contamination, dating, and sedimentation rates, Journal of Radioanalytical and Nuclear Chemistry, 307, 99-110, 2016.

Gälman, V., Rydberg, J., de-Luna, S. S., Bindler, R., and Renberg, I.: Carbon and nitrogen loss rates during aging of lake sediment: changes over 27 years studied in varved lake sediment, Limnology and Oceanography, 53, 1076-1082, 2008.

Grasset, C., Abril, G., Mendonça, R., Roland, F., and Sobek, S.: The transformation of macrophyte-derived organic matter to methane relates to plant water and nutrient contents, Limnology and Oceanography, 2019.

Grasset, C., Mendonça, R., Villamor Saucedo, G., Bastviken, D., Roland, F., and Sobek, S.: Large but variable methane production in anoxic freshwater sediment upon addition of allochthonous and autochthonous organic matter, Limnology and oceanography, 63, 1488-1501, 2018.

HydroBASINS: https://www.hydrosheds.org/page/hydrobasins, 2019.

Jenzer Althaus, J., De Cesare, G., Boillat, J.-L., and Schleiss, A.: Turbidity currents at the origin of reservoir sedimentation, case studies, Proceedings (on CD) of the 23rd Congress of the Int. Commission on Large Dams CIGB-ICOLD, 58-60, 2009.

Knoll, L. B., Vanni, M. J., Renwick, W. H., and Kollie, S.: Burial rates and stoichiometry of sedimentary carbon, nitrogen and phosphorus in M idwestern US reservoirs, Freshwater biology, 59, 2342-2353, 2014.

571 Kortelainen, P., Rantakari, M., Pajunen, H., Huttunen, J. T., Mattsson, T., Juutinen, S.,
572 Larmola, T., Alm, J., Silvola, J., and Martikainen, P. J.: Carbon evasion/accumulation
573 ratio in boreal lakes is linked to nitrogen, Global Biogeochemical Cycles, 27, 363-374,
574 2013.

575 Kunz, M. J., Anselmetti, F. S., Wüest, A., Wehrli, B., Vollenweider, A., Thüring, S.,
576 and Senn, D. B.: Sediment accumulation and carbon, nitrogen, and phosphorus
577 deposition in the large tropical reservoir Lake Kariba (Zambia/Zimbabwe), Journal of
578 Geophysical Research: Biogeosciences, 116, 2011.

579 Lehman, J. T.: Reconstructing the Rate of Accumulation of Lake Sediment: The Effect
580 of Sediment Focusing 1, Quaternary Research, 5, 541-550, 1975.

581 Liu, L., Wilkinson, J., Koca, K., Buchmann, C., and Lorke, A.: The role of sediment
582 structure in gas bubble storage and release, Journal of Geophysical Research:
583 Biogeosciences, 121, 1992-2005, 2016.

584 Maeck, A., DelSontro, T., McGinnis, D. F., Fischer, H., Flury, S., Schmidt, M., Fietzek,
585 P., and Lorke, A.: Sediment trapping by dams creates methane emission hot spots,
586 Environmental science & technology, 47, 8130-8137, 2013.

587 Maeck, A., Hofmann, H., and Lorke, A.: Pumping methane out of aquatic sediments:
588 Ebullition forcing mechanisms in an impounded river, Biogeosciences, 11, 2925-2938,
589 2014.

590 Marotta, H., Pinho, L., Gudasz, C., Bastviken, D., Tranvik, L. J., and Enrich-Prast, A.:
591 Greenhouse gas production in low-latitude lake sediments responds strongly to
592 warming, Nature Climate Change, 4, 467, 2014.

593 Mattson, M. D., and Likens, G. E.: Air pressure and methane fluxes. Nature, 347, 718,
594 1990.

595 McGinnis, D. F., Greinert, J., Artemov, Y., Beaubien, S., and Wüest, A.: Fate of rising
596 methane bubbles in stratified waters: How much methane reaches the atmosphere?,
597 Journal of Geophysical Research: Oceans, 111, 2006.

598 Mendonça, R., Kosten, S., Sobek, S., Barros, N., Cole, J. J., Tranvik, L., and Roland, F.:
599 Hydroelectric carbon sequestration, Nature Geoscience, 5, 838, 2012.

600 Mendonça, R., Kosten, S., Sobek, S., Cardoso, S. J., Figueiredo-Barros, M. P., Estrada,
601 C. H. D., and Roland, F.: Organic carbon burial efficiency in a large tropical
602 hydroelectric reservoir, Biogeosciences, 13, 3331-3342, 2016.

603 Mendonça, R., Kosten, S., Sobek, S., Cole, J. J., Bastos, A. C., Albuquerque, A. L.,
604 Cardoso, S. J., and Roland, F.: Carbon sequestration in a large hydroelectric reservoir:
605 an integrative seismic approach, Ecosystems, 17, 430-441, 2014.

606 Mendonça, R., Müller, R. A., Clow, D., Verpoorter, C., Raymond, P., Tranvik, L. J.,
607 and Sobek, S.: Organic carbon burial in global lakes and reservoirs, Nature
608 communications, 8, 1694, 2017.

609 Meyers, P. A., and Ishiwatari, R.: Lacustrine organic geochemistry—an overview of
610 indicators of organic matter sources and diagenesis in lake sediments, Organic
611 geochemistry, 20, 867-900, 1993.

612 Middelburg, J. J., Vlug, T., Jaco, F., and Van der Nat, W. A.: Organic matter
613 mineralization in marine systems, Global and Planetary Change, 8, 47-58, 1993.

614 Moreira-Turcq, P., Jouanneau, J., Turcq, B., Seyler, P., Weber, O., and Guyot, J.-L.:
615 Carbon sedimentation at Lago Grande de Curuai, a floodplain lake in the low Amazon
616 region: insights into sedimentation rates, Palaeogeography, Palaeoclimatology,
617 Palaeoecology, 214, 27-40, 2004.

618 Morris, G. L., and Fan, J.: Reservoir sedimentation handbook: design and management
619 of dams, reservoirs, and watersheds for sustainable use, McGraw Hill Professional,
620 1998.

621 Mulholland, P. J., and Elwood, J. W.: The role of lake and reservoir sediments as sinks
622 in the perturbed global carbon cycle, Tellus, 34, 490-499, 1982.

623 Paranaíba, J. R., Barros, N., Mendonça, R., Linkhorst, A., Isidorova, A., Roland, F.,
624 Almeida, R. M., and Sobek, S.: Spatially resolved measurements of CO2 and CH4
625 concentration and gas-exchange velocity highly influence carbon-emission estimates of
626 reservoirs, Environmental science & technology, 52, 607-615, 2018.

627 Prairie, Y. T., Alm, J., Beaulieu, J., Barros, N., Battin, T., Cole, J., Del Giorgio, P.,
628 DelSontro, T., Guérin, F., and Harby, A.: Greenhouse gas emissions from freshwater
629 reservoirs: what does the atmosphere see?, Ecosystems, 1-14, 2017.

630 Quadra, G. R., Lino, A., Sobek, A., Malm, O., Barros, N., Guida, Y., Thomaz, J.,
631 Mendonça, R., Cardoso, S., Estrada, C., Rust, F., and Roland, F.: Environmental Risk of
632 Metal Contamination in Sediments of Tropical Reservoirs. Bulletin of Environmental
633 Contamination and Toxicology, 1-10, 2019.

634 Radbourne, A. D., Ryves, D. B., Anderson, N. J., and Scott, D. R.: The historical
635 dependency of organic carbon burial efficiency, Limnology and Oceanography, 62,
636 1480-1497, 2017.

637 Raymond, P. A., Hartmann, J., Lauerwald, R., Sobek, S., McDonald, C., Hoover, M.,
638 Butman, D., Striegl, R., Mayorga, E., and Humborg, C.: Global carbon dioxide
639 emissions from inland waters, Nature, 503, 355, 2013.

640 Renwick, W. H., Smith, S. V., Bartley, J. D., and Buddemeier, R. W.: The role of
641 impoundments in the sediment budget of the conterminous United States.
642 Geomorphology, 71, 99-111, 2005.

643 Sanders, L. M., Taffs, K. H., Stokes, D. J., Sanders, C. J., Smoak, J. M., Enrich-Prast,
644 A., Macklin, P. A., Santos, I. R., and Marotta, H.: Carbon accumulation in Amazonian
645 floodplain lakes: A significant component of Amazon budgets?, Limnology and
646 Oceanography Letters, 2, 29-35, 2017.

647 Schleiss, A. J., Franca, M. J., Juez, C., and De Cesare, G.: Reservoir sedimentation,
648 Journal of Hydraulic Research, 54, 595-614, 2016.

649 Scully, M., Friedrichs, C. T., and Wright, L.: Numerical modeling of gravity-driven
650 sediment transport and deposition on an energetic continental shelf: Eel River, northern
651 California, Journal of Geophysical Research: Oceans, 108, 2003.

652 Sedláček, J., Bábek, O., and Kielar, O.: Sediment accumulation rates and high-
653 resolution stratigraphy of recent fluvial suspension deposits in various fluvial settings,
654 Morava River catchment area, Czech Republic, Geomorphology, 254, 73-87, 2016.

655 Sikar, E., Matvienko, B., Santos, M., Rosa, L., Silva, M., Santos, E., Rocha, C., and
656 Bentes Jr, A.: Tropical reservoirs are bigger carbon sinks than soils, Internationale
657 Vereinigung für theoretische und angewandte Limnologie: Verhandlungen, 30, 838-
658 840, 2009.

Sobek, S., DelSontro, T., Wongfun, N., and Wehrli, B.: Extreme organic carbon burial fuels intense methane bubbling in a temperate reservoir, Geophysical Research Letters, 39, 2012.

Sobek, S., Durisch-Kaiser, E., Zurbrügg, R., Wongfun, N., Wessels, M., Pasche, N., and Wehrli, B.: Organic carbon burial efficiency in lake sediments controlled by oxygen exposure time and sediment source, Limnology and Oceanography, 54, 2243-2254, 2009.

Sobek, S., Zurbrügg, R., and Ostrovsky, I.: The burial efficiency of organic carbon in the sediments of Lake Kinneret, Aquatic sciences, 73, 355-364, 2011.

Stratton, L. E., Haggerty, R., and Grant, G. E.: The Importance of Coarse Organic Matter and Depositional Environment to Carbon Burial Behind Dams in Mountainous Environments. Journal of Geophysical Research: Earth Surface, 124, 2118-2140, 2019.

Syvitski, J. P., and Kettner, A.: Sediment flux and the Anthropocene. Philosophical Transactions of the Royal Society A: Mathematical, Physical and Engineering Sciences, 369, 957-975, 2011.

Teodoru, C. R., Bastien, J., Bonneville, M. C., del Giorgio, P. A., Demarty, M., Garneau, M., Hélie, J. F., Pelletier, L., Prairie, Y. T., and Roulet, N. T.: The net carbon footprint of a newly created boreal hydroelectric reservoir, Global Biogeochemical Cycles, 26, 2012.

Tranvik, L. J., Downing, J. A., Cotner, J. B., Loiselle, S. A., Striegl, R. G., Ballatore, T. J., Dillon, P., Finlay, K., Fortino, K., and Knoll, L. B.: Lakes and reservoirs as regulators of carbon cycling and climate, Limnology and Oceanography, 54, 2298-2314, 2009.

682 Verpoorter, C., Kutser, T., Seekell, D. A., and Tranvik, L. J.: A global inventory of
683 lakes based on high-resolution satellite imagery, Geophysical Research Letters, 41,
684 6396-6402, 2014.

685 Vörösmarty, C. J., Meybeck, M., Fekete, B., Sharma, K., Green, P., and Syvitski, J. P.:
686 Anthropogenic sediment retention: major global impact from registered river
687 impoundments, Global and planetary change, 39, 169-190, 2003.

688 Wik, M., Thornton, B. F., Bastviken, D., MacIntyre, S., Varner, R. K., and Crill, P. M.:
689 Energy input is primary controller of methane bubbling in subarctic lakes, Geophysical
690 Research Letters, 41, 555-560, 2014.

691 Winemiller, K. O., McIntyre, P. B., Castello, L., Fluet-Chouinard, E., Giarrizzo, T.,
692 Nam, S., Baird, I., Darwall, W., Lujan, N., and Harrison, I.: Balancing hydropower and
693 biodiversity in the Amazon, Congo, and Mekong, Science, 351, 128-129, 2016.

694 Yvon-Durocher, G., Allen, A. P., Bastviken, D., Conrad, R., Gudasz, C., St-Pierre, A.,
695 Thanh-Duc, N., and Del Giorgio, P. A.: Methane fluxes show consistent temperature
696 dependence across microbial to ecosystem scales, Nature, 507, 488, 2014.

697 Zarfl, C., Lumsdon, A. E., Berlekamp, J., Tydecks, L., and Tockner, K.: A global boom
698 in hydropower dam construction, Aquatic Sciences, 77, 161-170, 2015.

699 Zhang, Y., Xiao, X., Wu, X., Zhou, S., Zhang, G., Qin, Y., and Dong, J.: A global
700 moderate resolution dataset of gross primary production of vegetation for 2000–2016,
701 Scientific data, 4, 2017.